

The results of the first photonuclear reaction performed in Turkey: the zinc example

İsmail BOZTOSUN^{1,2,*}, Haris –DAPO^{1,2}, Süleyman Fatih ÖZMEN^{1,2}, Yiğit ÇEÇEN^{2,3},
Mesut KARAKOÇ^{1,2}, Abdullah ÇOBAN¹, Alp CESUR¹, Tanfer CANER¹, Edip BAYRAM^{2,4},
Gizem Büşra KELLER¹, Beyza KÜÇÜK¹, Abdullah GÜVENDİ¹, Melek DERMAN¹, Deniz KAYA^{1,2}
¹Department of Physics, Akdeniz University, Antalya, Turkey
²Nükleer Bilimler Uygulama ve Araştırma Merkezi, Akdeniz University, Antalya, Turkey
³Department of Radiation Oncology, Akdeniz University, Antalya, Turkey
⁴Department of Chemistry, Akdeniz University, Antalya, Turkey

Received: 29.05.2013 • Accepted: 22.08.2013 • Published Online: 17.01.2014 • Printed: 14.02.2014

Abstract: We have investigated the decays of several zinc isotopes produced by photonuclear reactions, which were induced by bremsstrahlung photon beams from a clinical e-linac. A photon beam of 18 MeV endpoint energy was directed at a target consisting of primarily zinc isotopes in their natural abundances. Subsequently, the induced decays of unstable zinc isotopes were measured with an HPGe detector twice, once shortly after irradiation and once on the following day. Decays of Zn-63, Zn-65, Zn-69m, and Cu-67 were measured and fitted. In addition, the gamma energy levels of the daughters of these decays were measured with good accuracy. All of the measurements were consistent with established data within error bars.

Key words: Photonuclear reaction, photoactivation, knock-out reactions, energy levels, radioactive decay, e-linac accelerator

1. Introduction

In the past, photoactivation experiments involving linear accelerators have been performed at several institutions around the world [1, 2], and in one of the latest approaches [3], a clinical linac was employed. These medical accelerators, which are capable of producing bremsstrahlung photons with endpoint energies of up to 25 MeV, are nowadays a part of the radiation treatment facilities of many hospitals. It is interesting to note that such linacs compare well to the linacs made for physics experiments such as the S-DALINAC at TU Darmstadt, ELBE at Forschungszentrum Dresden in Rossendorf, or commercially available electron accelerators.

The pioneering experiment of [3] has shown that clinical linear accelerators (cLINACs) are able to provide sufficient photon intensity for photoactivation experiments. Such experiments are often motivated by astrophysical references to nucleosynthesis processes where such energies of up to 10 MeV are occasionally present; see [4, 5, 6, 7, 8, 9, 10] and references therein.

In the present experiment, we have employed a setup with a cLINAC to perform a photoactivation experiment with stable zinc isotopes. The motivation for using well-known, stable isotopes on which these kinds of measurements were performed decades ago in the United States and Europe may be explained as follows: since this is the first such experiment carried out by our group, it is essential to establish reliable experimental

*Correspondence: boztosun@akdeniz.edu.tr

procedures, capable of reproducing already measured results. In this way, we can gain new understanding of technology, carry out practices beyond the scope of such measurements, and prepare ourselves for future goals. In any event, this is an important milestone both for us as an institution and for Turkey in general, as this is the first time such experiments have been performed entirely and independently by a Turkish scientific institution. It is also worth noting that most of the data pertaining to these reactions actually come from the inverse of the reaction studies here. Namely, the data primarily come from neutron absorption and subsequent decay while we perform neutron separation and study the subsequent decay.

The paper is organized as follows: in Section 2, we will explain the experimental procedures involved in performing the experiment. Section 3 will present the results and data analysis, while in Section 4, we set out the conclusions.

2. Experimental Procedure

The cLINAC that was used as a source of photons is a standard and up-to-date Elekta TM Synergy TM accelerator, whose technical documentation can be found in [11]. The accelerator's primary electron beam is generated by a gun with an energy of 50 keV. The electrons are accelerated in a copper cavity by 30 GHz radio frequency with peak power of about 5 MW. For an electron energy of about 10 MeV, the typical average electron current is about 300 μ A. Figure 1 shows the schematic view of the cLINAC.

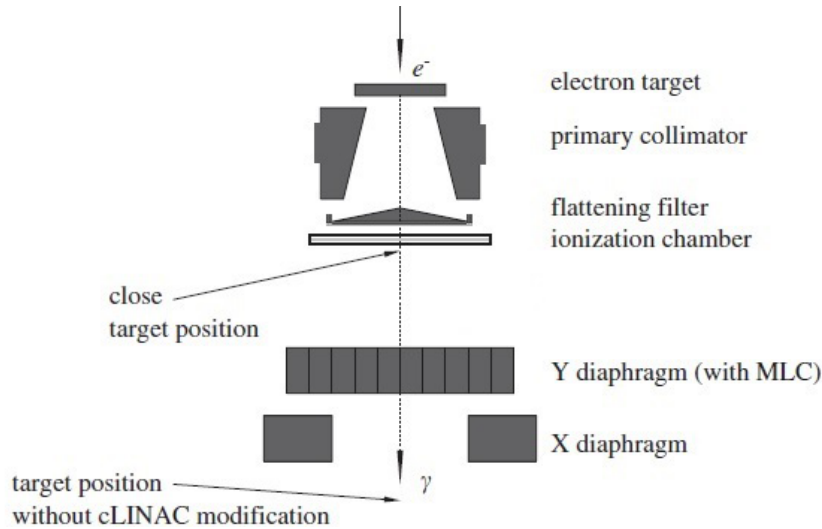


Figure 1. Schematic view of the photon beam production at the cLINAC.

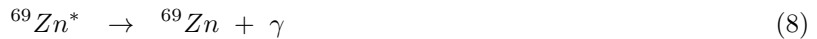
Steering and focusing of the beam is achieved by standard magnetic and electrostatic devices. At the end, the electron beam is aimed at the tungsten target, which stops the electrons, thus producing photons via bremsstrahlung. As usual, the endpoint energy of the beam corresponds to the energy of the electrons before the impact. The bremsstrahlung photons are collimated and flattened with several filters, resulting in a uniform forward focused photon beam. This is done as the standard procedure for delivering a uniform dose to the patient. In this way, the collimated and flattened beam is also collimated in the horizontal direction such that, at a distance of 100 cm, the maximum area covered by photons is $40 \times 40 \text{ cm}^2$. For patient purposes, the area can be made into an irregular shape with additional collimators.

In this experiment, we used a metallic target made of 67% zinc by mass fraction with natural abundances of zinc isotopes. Within that 67%, present as usual were ^{64}Zn at 49.17%, ^{66}Zn at 27.17%, ^{67}Zn at 4.04%, ^{68}Zn

at 18.45%, and ^{70}Zn at 0.61%. The sample had a total weight of 10.6 g, a thickness of 1 mm, and $5 \times 5 \text{ cm}^2$ size. It was placed at 58 cm in distance from the source (SSD). The sample was bombarded with photons, whose endpoint energy was 18 MeV. Since the neutron separation energy of the aforementioned zinc isotopes is in the range of 7 to 12 MeV and the proton separation energy is in the range of 7.5 to 11.5 MeV, all photoneutron and photoproton reactions with these elements are, in principle, possible. The total irradiation time was 1 h. After the irradiation, no chemical purification was attempted.

In order to measure the spectra of the samples, they were placed into a well-shielded, high-purity germanium detector (HPGe). The sample was placed into the detector 15 min after irradiation for 30 min. The second measurement was performed for 24 h, 1 day after original irradiation. The detector used was a p-type, coaxial, electrically cooled, HPGe gamma-ray spectrometer AMATEK-ORTEC (GEM40P4-83) with 40% relative efficiency and 768 eV FWHM at 122 keV for ^{57}Co and 1.85 keV FWHM at 1332 keV for ^{60}Co [12]. It was connected to a NIM consisting of ORTEC bias supply, a spectroscopy amplifier, an analog-to-digital converter, and a computer. The detector was placed into a 10-cm-thick lead shield with an inner surface covered by a 2-mm-thick copper foil to shield it from the X-rays originating in lead. Data acquisition was carried out with MAESTRO32 software. A mixed calibration source supplied by the Çekmece Nuclear Research and Training Center (IAEA 1364-43-2) emitting gamma rays in the energy range between 47 and 1836 keV was used for energy calibration. The detector was configured with 8192 channels having channel width of 0.33954 keV.

Although many reactions were possible under the chosen energy conditions, it was possible to observe only a handful due to experimental restrictions. The primary experimental constraint was the off-line nature of our measurements, which allowed observations only for elements whose half-lives were of the order of 10 min. Any shorter half-lives were not expected to be observed. This immediately ruled out any reaction resulting in a stable element even if it were in an excited state, since most γ -decay half-lives are extremely short. One exception is the metastable state of ^{69}Zn , whose half-life is almost 14 h, which was observed and was included in our considerations. The experimental restrictions also prevented us from observing the decay of ^{66}Cu , since its half-life is only 5 min. The very weak branching ratios of some processes and the great majority of decays going straight to the ground state rather than to an excited state were the other restrictions. In this case, we were unable to observe any γ -level transitions and hence were not able to detect the half-lives of the parent nucleus. Given all of these constraints, the few processes that were observable were as follows.





Several other reactions involving ${}^{69}\text{Zn}$ and ${}^{66}\text{Zn}$ were likely to have happened, but due to overly short lifetimes and small branching ratios, they could not be observed.

3. Results and data analysis

In the following, we show the results of our data acquisition and analysis. All spectra were analyzed by RadWare code, which is a package for analysis of gamma-ray coincidence data, developed by David Radford of the Physics Division at Oak Ridge National Laboratory and freely available from <http://radware.phy.ornl.gov>. The counts representing the peaks were fitted as part of the RadWare analysis with a Gaussian, a skewed Gaussian, and a smoothed step function. In this way, we determined the energies of the transitions creating these peaks. In addition, the analysis provided us with the net counts under the peaks. We used least-squares to fit the net counts assigned to peaks in order to determine the decay rates of the parent nuclei. In our analysis, we realized that it was more favorable to fit the net area directly with a function of $\Delta N(t) = N_0(1 - \exp(-\lambda t))$ rather than using the activity $A(t) = A_0 \exp(-\lambda t)$. Once the value of the decay constant λ was obtained, it was a straightforward matter to calculate the half-lives $T_{1/2} = \ln 2 / \lambda$. We also noted that all the error bars quoted were only statistical.

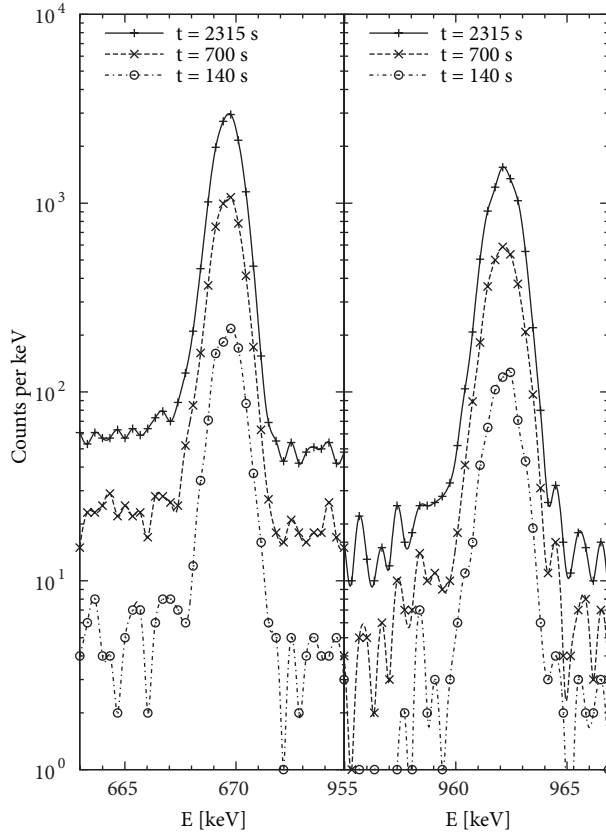


Figure 2. γ -rays of ${}^{63}\text{Cu}$ observed using HPGe 3 different times. On the left, 660 to 675 keV, and on the right, 955 to 970 keV. In both panels, only one peak has been focused on.

Figure 2 shows the γ -ray spectra from the source counted shortly after the irradiation. This measurement focused on the short-lived isotopes only when the presence of ^{63}Cu was confirmed. The 2 identifying peaks are shown in Figure 2. On the left side, the peak at 669 keV is shown, while on the right side, one sees the 962 keV peak. From nuclear data sheets [13], these peaks are identified as 669.62 ± 0.05 keV and 962.06 ± 0.04 keV belonging to ^{63}Cu . In our experiment, we measured these 2 peaks as 669.58 ± 0.02 keV and 962.10 ± 0.02 keV, which have very good overlap with the documented results. In fact, it is quite astonishing that one could achieve such accuracy with an offline set-up, which is relatively simple compared to the usually employed multidetector online setups.

The spectra in Figure 2 show 3 different counting times. The net area was calculated from the fit of the data. The resulting sums of counts for those 3 counting times and several more are displayed in Figure 3. For Figure 3 we can see the temporal dependence of the count. If these data are fitted by $\Delta N(t) = N_0[1 - \exp(-\lambda t)]$ with no input from theory, we can deduce the half-life of the parent nucleus, which in this case is ^{63}Zn . The fitted results are 40.8 ± 0.6 min from the 669 peak and 34.6 ± 0.7 min from the 962 peak, which are not far from the expected value of 38.47 ± 0.05 min from the nuclear data sheets [13], and even more so if we calculate the combined value of these 2 measurements as 37.7 ± 0.9 min. The results for the half-life are as good as those for the energy and are reasonable.

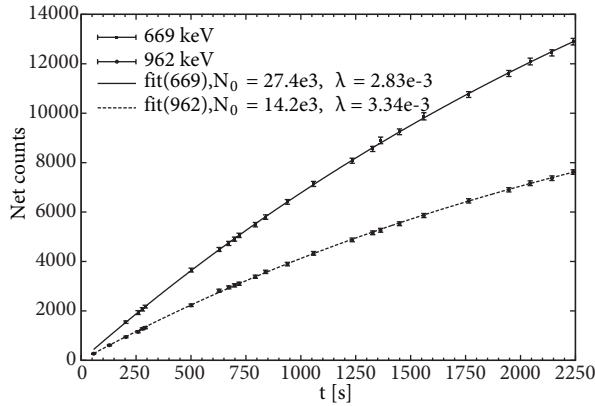


Figure 3. Net area change with time, i.e. decay curve of the activity, of ^{63}Cu for 669 keV and 930 keV transitions and corresponding fits. The new results and accepted NDS data are listed in the text.

The second measurement of the sample, which was performed 1 day after the irradiation, was aimed at isotopes with a longer half-life and, indeed, we detected the presence of 3 more. An example of the first can be seen in Figure 4. There we show the 184 keV transition on the left side and the 300 keV transition of ^{67}Zn coming from the β -decay of ^{67}Cu created by proton separation of ^{68}Zn as in Eq. (9) through Eq. (11). According to the nuclear data sheets [14], these transition energies are 184.577 ± 0.010 keV and 300.219 ± 0.010 keV. From our measurements, we obtained the values of 184.273 ± 0.005 keV and 300.04 ± 0.23 keV, respectively. The resulting decay curves are shown in Figure 5, giving 60.3 ± 0.6 h from the 184 keV transition and 197 ± 73 h from the 300 keV transition, while the expected value for the half-life of ^{67}Cu is 61.83 ± 0.12 h [14]. As can be seen in both cases, the 184 keV transition gives better results since it is much stronger, i.e. it has a much greater net area than the 300 keV transition. In fact, the transition was so weak in comparison to that of 184 keV that in Figure 5 we had to multiply it by a factor of 50 to make it visible on the same graph.

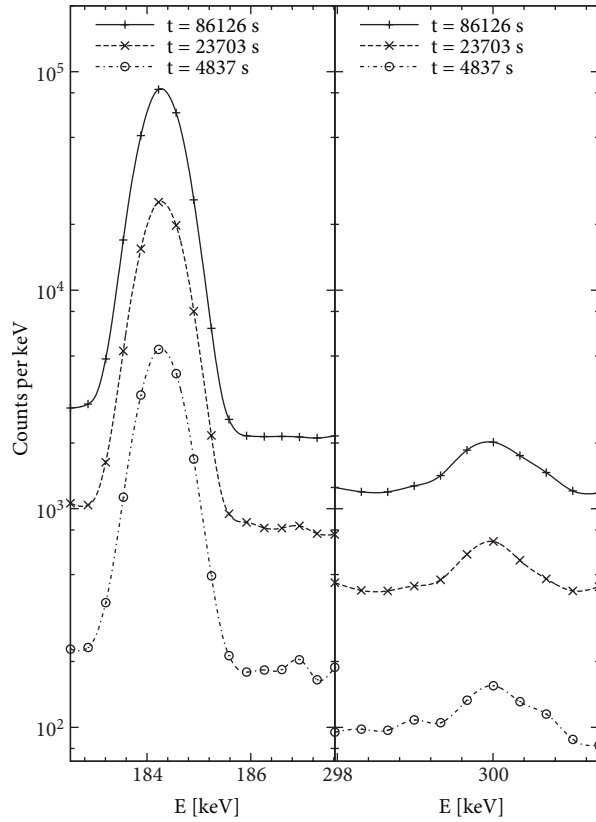


Figure 4. γ -rays of ^{67}Zn were observed using HPGe for 3 different counting times. On the left, 182 to 188 keV, and on the right, 298 to 302 keV. In both panels, only one peak has been focused on.

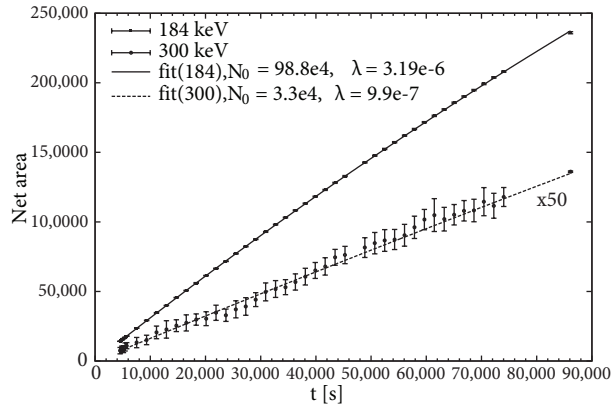


Figure 5. Net area change with time, i.e. decay curve of the activity, of ^{67}Cu for 184 keV and 300 keV transitions and corresponding fits. The results and fit for 300 keV transitions have been multiplied with a factor of 50, as labeled in the figure, in order to make them more visible. The new results and accepted NDS data are listed in the text.

Other transitions in ^{67}Zn were also detected with similar accuracies. However, due to their small energies, their counts were polluted by the multiisotope nature of the target. Due to this pollution, it was impossible to fit them with just one decay constant.

The other 2 transitions are shown in Figure 6. On the left side, we show the 438 keV metastable state of ^{69}Zn , while, on the right side, one can observe the 1115 keV state of ^{65}Cu . The defining decays of the

parent nuclei are shown in Eq. (4) through Eq. (6) for ^{69}Zn and Eq. (7) through Eq. (8) for ^{65}Cu . The quoted energy value from nuclear data sheets [15, 16] for the 438 keV transition is 438.614 ± 0.018 , while for 1115, it is 1115.546 ± 0.004 keV. In our measurements, we obtained somewhat lower results of 438.512 ± 0.005 and 1115.696 ± 0.008 keV, respectively. Since our statistical errors are in fact better than the quoted errors of the nuclear data sheets, the only possible source of this discrepancy is due to unknown systematic errors. Unfortunately, it was not clear where such errors came from. However, even if one considers errors large enough to have overlapping error bars of the order of 0.1 keV, we are still reasonably close to the expected value. Once again, given the crudeness of this very first experiment conducted at our facility, this is not a disappointing result.

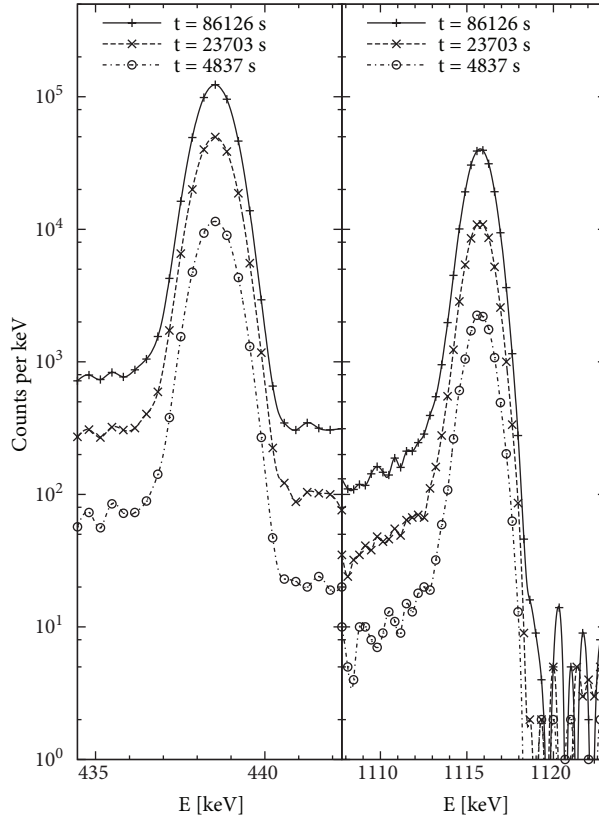


Figure 6. γ -rays observed using HPGe for 3 different counting times. On the left, 434 to 442 keV, and on the right, 1105 to 1125 keV. In both panels, only one peak has been focused on. The left peak has been assigned to ^{69}Zn , while the right peak has been assigned to ^{65}Cu .

In Figure 7 we show the decay curve of ^{70}Zn , the parent nucleus of ^{69}Zn . The result obtained by the fit is 13.51 ± 0.03 h, while the expected value is 13.74 ± 0.02 h [15]. As for the transition level, there is a discrepancy; but, unlike before, this systematic error is well understood in terms of the multiisotope nature of our sample where the presence of isotopes with different half-lives leads to changes in the net area time dependence. Given this, we were able to get within 5% of the correct half-life, which is a good achievement. Moreover, this observation of ^{69}Zn evidently leads to the conclusion that ^{69}Ga was also produced, even though we were unable to confirm this with detection of any ^{69}Ga transitions.

In Figure 8, we show the net area time dependence of the 1115 keV peak of ^{65}Cu . Since this peak is the result of the decay of ^{64}Zn , the expected half-life from nuclear data sheets [16] is 243.93 ± 0.09 days, and since our observation time was only 1 day, it was impossible to fit the curve as the exponent. What could be fitted and what we did fit was a first term in the Taylor series of $\Delta N(t) = N_0[1 - \exp(-\lambda t)] \approx N_0 \cdot \lambda t$. By this way, instead of independently fitting N_0 and λ as before, we get their product. The value of it was $N_0 \cdot \lambda = 2.462 \pm 0.001$ 1/s.

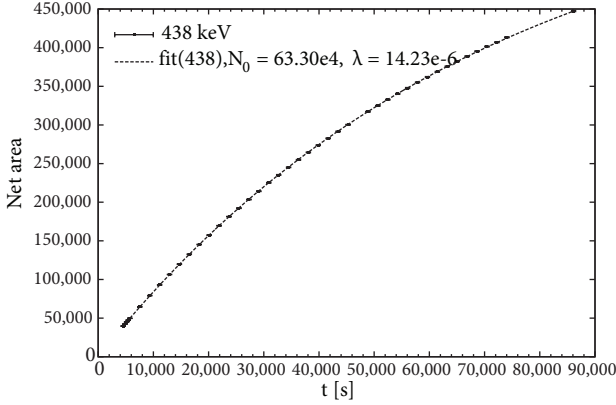


Figure 7. Net area change with time, i.e. decay curve of the activity, of ^{69}Cu for 438 keV transitions and corresponding fit. The new results and accepted NDS data are listed in the text.

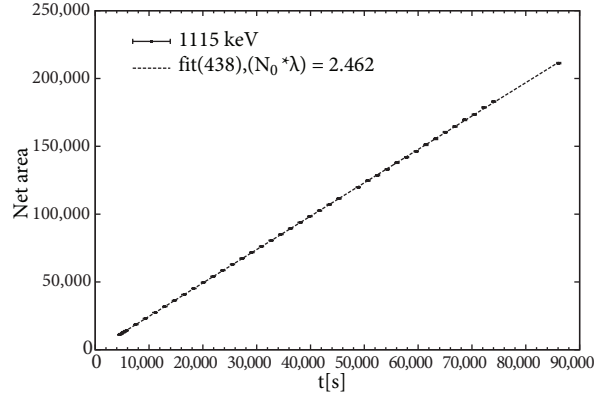


Figure 8. Net area change with time, i.e. decay curve of the activity, of ^{65}Cu for 1115 keV transitions and corresponding fit. The new results and accepted NDS data are listed in the text.

4. Summary and conclusion

The goal of this work was to investigate the spectra and half-lives of Zn isotopes and of their daughter nuclei, created through photonuclear reactions. The radioactivity was induced by the photon beam separating neutrons or protons from their nuclei. In order to have sufficient energies for such a process to occur, the photon beam was produced by electrons of 18 MeV produced by a cLINAC accelerator impacting on a tungsten target. The bremsstrahlung photons, with an endpoint energy of 18 MeV, were sufficiently energetic to achieve photonuclear reactions with a Zn target.

The target contained multiple Zn isotopes in their natural abundances. Hence, several different radioactive isotopes were produced. Their decay was observed by detecting the gamma transition of their daughter nuclei. Thus, 2 quantities were extracted. One was the energy spectrum of the daughter nuclei and the other was the decay rate, i.e. the half-life, of the parent nucleus. The quantities in question were measured and the results were compared to the expected values from the nuclear data sheets. As we have shown, most of the results agreed well, and especially so if one takes into account our limitations. It was even surprising that, for several gamma transitions, our results compared very well with expected values; for example, the cases of ^{63}Cu and all others were within 1% or better of expected values.

For the half-life results, the agreement was not so consistent, but with ^{69}Zn , we demonstrated that we could get very close to the expected values. In addition, as we noted in this paper, technically speaking, our results are in a way unique, since none of the results quoted in the nuclear data sheets come from photonuclear reactions; rather, most of them come from the inverse reaction, i.e. neutron capture. This is an understandable situation since the majority of the decay data for the nuclei investigated come from the late 1960s and early 1970s, when these kinds of experiments were being performed by placing samples in reactor cores.

In conclusion, in this paper, we have shown the results of the first photonuclear reaction performed in Turkey. Even though the quantities measured in this experiment had previously been determined in other experiments, it is nevertheless a significant achievement for Akdeniz University in particular and for Turkey in general to have reached such an important experimental milestone. The significance is 2-fold: on one hand, we have achieved, with limited time and resources, a result that, for the most part, is within 10% of the expected values. On the other hand, we have also gained crucial experimental nuclear physics knowledge and know-how previously lacking at Akdeniz University and very poorly distributed even across the whole of Turkey. With this challenge achieved, we feel that we are ushering a new era in Turkey's experimental nuclear physics research and we certainly intend to continue this line of work, hopefully with even better results to be presented in the future.

Acknowledgments

We would like to thank the Akdeniz University Hospital for its generous support in providing us with necessary hardware to perform this experiment, as well as a very welcoming policy regarding access to facilities. This project also received administrative support from the Akdeniz University Rectorate. In addition, the project and its various contributors were in part supported by a TÜBİTAK-TBAG 111T275 grant via the 2216 Foreigner Research Program.

References

- [1] Guildford, J. *Radioanal. Nucl. Chem., Proceedings of the 11th International Conference on Modern Trends in Activation Analysis (MTAA - 11)*, Surrey, 271, 2007.
- [2] Masumoto, K.; Segebade, C. *Photon Activation Analysis* **2006**, DOI: 10.1002/9780470027318.a6211.pub2.
- [3] Mohr, P.; Brieger, S.; Witucki, G.; Maetz, M. *Nucl. Instrum. Meth.* **2007**, *A580*, 1201–1208.
- [4] Webb, T.; DeVeaux, L.; Harmon, F.; Petrisko, J.; Spaulding, R. *Conf. Proc.* **2005**, *C0505161*, 2363.
- [5] Meyer, B.; Mathews, G.; Howard, W.; Woosley, S.; Ho_man, R. *Astrophys. J.* **1992**, *399*, 656–664.
- [6] Lambert, D. *Astron. Astrophys. Rev.* 1992, *3*, 201–256.
- [7] Rauscher, T.; Heger, A.; Ho_man, R.; Woosley, S. *Astrophys. J.* **2002**, *576*, 323.
- [8] Arnould, M.; Goriely, S. *Phys. Rep.*, 2003, *384*, 1–84.
- [9] Hayakawa, T.; Iwamoto, N.; Shizuma, T.; Kajino, T.; Umeda, H.; Nomoto, K. *Phys. Rev. Lett.* **2004**, *93*, 161102–161106.
- [10] Utsunomiya, H.; Mohr, P.; Zilges, A.; Rayet, M. *Nucl. Phys.* **2006**, *A777*, 459–478.
- [11] Elekta Digital Accelerator, Technical Training Guide, **2003** (unpublished).
- [12] MAESTRO, **2012**, URL <http://www.ortec-online.com/download/A65-B32-MAESTRO-32-Emulation-Software.pdf>.
- [13] Erjun, B.; Junde, H. *Nuclear Data Sheets* **2001**, *92*, 147–251.
- [14] Browne, E.; Tuli, J. *Nuclear Data Sheets* **2010**, *111*, 2425–2553.
- [15] Junde, H.; Xiaolong, H.; Tuli, J. *Nuclear Data Sheets* **2005**, *106*, 159–250.
- [16] Bhat, M. *Nuclear Data Sheets* **1989**, *58*, 1–91.